

## Photocatalytic Activity of Metal Ion (Fe or W) Doped Titania

Sang Soo Lee, Hyun Jong Kim, Kyung Taek Jung, Hak Soo Kim\* and Yong Gun Shul†

Department of Chemical Engineering, Yonsei University, Seoul 120-749, Korea

\*Department of Chemical Engineering, Sunmoon University, Chung-nam 336-708, Korea

(Received 7 September 2001 • accepted 13 October 2001)

**Abstract**—Iron or tungsten-doped nano  $\text{TiO}_2$  were successfully synthesized from  $\text{TiCl}_4$ . All of the samples showed anatase phase of  $\text{TiO}_2$ . For the iron-doped  $\text{TiO}_2$ , Iron ion was well dispersed in the  $\text{TiO}_2$  lattice. However, tungsten-doped  $\text{TiO}_2$  formed 12-tungstate with anatase  $\text{TiO}_2$ . As the concentration of tungsten increased, 12-tungstate disappeared. The photocatalytic oxidation of acetaldehyde was evaluated to examine the photocatalytic characteristics of metal-doped  $\text{TiO}_2$ . Because of the surface containing metal oxide or metal precursors at high concentration metal ion, increasing the concentration of W or Fe ion decreased the reactivity. The reaction rate was drastically increased after 300 °C heat treatment. Furthermore, the photocatalytic activity of iron- or tungsten-doped  $\text{TiO}_2$  was higher than that of synthesized pure  $\text{TiO}_2$  and commercial  $\text{TiO}_2$ .

Key words: Photocatalysis, Photocatalyst,  $\text{TiO}_2$ , Metal-Doped  $\text{TiO}_2$

### INTRODUCTION

Photocatalytic oxidation of volatile organic compounds in water and air has received much attention as a potential technology of pollution abatement. Heterogeneous photocatalysis is the ambient temperature process in which the surface of an illuminated semiconductor acts as a chemical reaction catalyst by using band gap light. These semiconductor compounds usually have a moderate energy band gap (1-3.7 eV) between their valence and conduction bands. The semiconductor photocatalyst for the reaction must be (1) photoactive; (2) able to utilize visible and/or near-UV light; (3) biologically and chemically inert; (4) photostable, i.e., not liable to photoanodic corrosion for example; (5) inexpensive [Mills et al., 1997]. By common consent, the  $\text{TiO}_2$  satisfies criteria (1)-(5) and is one of the best semiconductors for photocatalytic reactions. Many researchers have proved that  $\text{TiO}_2$  is an excellent photocatalyst that can break down most kinds of refractory organic pollutants, including detergents, dyes, pesticides and herbicides under UV-light irradiation [Linsebigler et al., 1995].

Although  $\text{TiO}_2$  is the most useful photocatalyst, the search for new materials in heterogeneous photocatalysis continues to be a matter of interest at the present. Doping of titania with transition metal ions has been tested as a promising way of improving the photocatalytic activity of  $\text{TiO}_2$ . The benefit of transition metal doping species is the improved trapping of electrons to inhibit electron-hole recombination during illumination. The presence of metal ions determines the formation of a permanent space charge region whose electric force improves the efficiency of hole-electron separation and consequently the charge transfer [Palmisano et al., 1997]. From a chemical point of view, moreover, it should be also observed that metal ion-doped  $\text{TiO}_2$  is equivalent to the introduction of defects, i.e.,  $\text{Ti}^{3+}$  in the lattice. However, the reactivity of doped  $\text{TiO}_2$  appears to be a complex function of the dopant concentration, the en-

ergy level of the dopants within the  $\text{TiO}_2$  lattice, their d-electronic configuration, the distribution of dopants, the electron-donor concentration, and the light intensity [Hoffmann et al., 1995]. Some brief mentions to this subject have appeared in the literature, but there does not exist a complete and exhaustive revision [Litter et al., 1996].

In this paper, titania particles were prepared from  $\text{TiCl}_4$ . The use of inorganic salt precursor rather than organic alkoxide precursor not only can reduce the cost of synthesis, but also can avoid the use of organic solvent to decrease pollution. And, we doped the iron or tungsten ion on the  $\text{TiO}_2$  particles to improve the photocatalytic characteristics. Photodegradation of acetaldehyde was tested to examine a number of preparation variables which affect the photocatalytic activity of Fe- or W-doped  $\text{TiO}_2$  catalyst.

### EXPERIMENTAL

#### 1. Catalyst Preparation

$\text{TiO}_2$  and metal doped titania were prepared by precipitation method using titanium tetrachloride ( $\text{TiCl}_4$ , Aldrich Co.), iron trichloride hexahydrate ( $\text{FeCl}_3 \cdot 6\text{H}_2\text{O}$ , Aldrich Co.), and tungsten tetrachloride ( $\text{WCl}_6$ , Aldrich Co.).  $\text{FeCl}_3 \cdot 6\text{H}_2\text{O}$  or  $\text{WCl}_6$  was dissolved into distilled water and kept below 1 °C.  $\text{TiCl}_4$  was added drop-wisely to the aqueous solution to suppress the active hydrolysis reaction. For the case of pure  $\text{TiO}_2$ ,  $\text{TiCl}_4$  was slowly dropped directly to water.

The obtained suspensions were kept in cooling bath for 1 hour to create photocatalyst particles with constant stirring. The solution was then dialyzed by using Spectra/Por (MWCO:6-8000) membrane. After the removal of solvent by using a rotary vacuum evaporator, the solid was calcined at various temperatures (100-500 °C) in open air for 7 hours.

#### 2. Reactivity Measurement

Photocatalytic decomposition of gaseous acetaldehyde was examined by measuring the concentration of acetaldehyde as a function of irradiation time under UV light illumination with two 6 W fluorescent lamp. Fig. 1 shows the apparatus for measurement of photocatalytic activity. The gaseous reaction was carried out in a

\*To whom correspondence should be addressed.

E-mail: shulg@yonsei.ac.kr

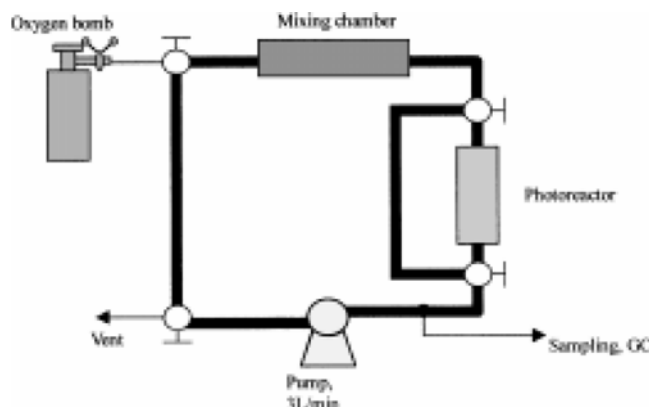


Fig. 1. Experimental apparatus for measurement of photocatalytic activity.

film type quartz reactor, which is equipped with a gas recirculation system. Acetaldehyde was fed with a saturator as the liquid, which was completely evaporated and mixed with  $O_2$  prior to entering the reactor. The inlet concentration of acetaldehyde was 500 ppm. Irradiation was conducted at room temperature after the equilibrium between gaseous and adsorbed reactants was achieved. Finally, the concentration of acetaldehyde was analyzed by gas chromatography (Shimadzu GC-8A, Porapak T column) with a flame ionization detector (FID).

### 3. Analysis Methods

The size of  $TiO_2$  and metal doped  $TiO_2$  was measured by the dynamic light scattering method using a light scattering measuring apparatus (Brookhaven Particle Sizer, Zetaplus). To determine the crystal phase of the prepared  $TiO_2$  and metal doped  $TiO_2$ , X-ray powder diffraction (XRD) was measured on a Rigaku X-ray diffractometer with  $Cu K\alpha$  radiation source. Raman spectrum was also analyzed by using a Raman spectrometer (Jobin Yvon T64000) with Ar laser.

## RESULTS AND DISCUSSION

The mean particle sizes for the pure and metal doped  $TiO_2$  are shown in Table 1. The size distribution of the  $TiO_2$  particles was uniform and the most probable particle size was about 6 nm. It is reasonable to ignore the effects of particle size on crystallographic results and photocatalytic activity.

Fig. 2 shows the XRD spectra of iron-doped  $TiO_2$ . All of the titania prepared at room temperature in this system were in the anatase form. Although the content of Fe ion was increased up to 10 mol%, any crystalline phase which was related with Fe complex could not be found. In the Raman spectra of Fig. 3, however, some additional peaks except the  $TiO_2$  phase were detected. In above 10 mol% Fe/  $TiO_2$  samples, peaks of 108 and 333  $cm^{-1}$  were attributed to  $FeCl_3$ ,

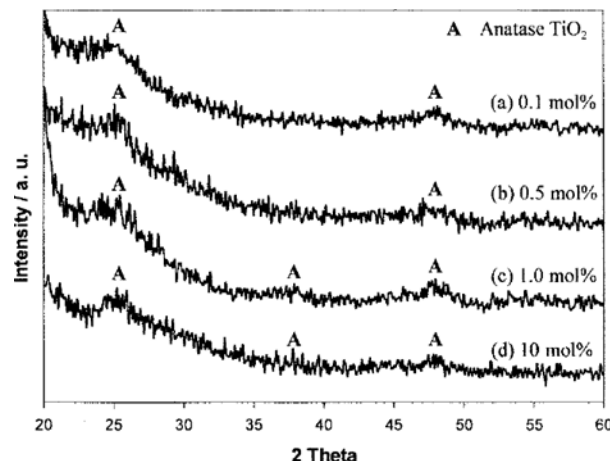


Fig. 2. XRD spectra of (a) 0.1, (b) 0.5, (c) 1 and (d) 10 mol% Fe doped  $TiO_2$ .

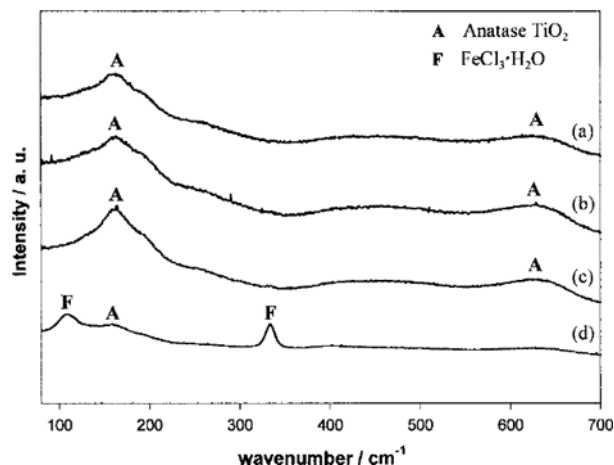


Fig. 3. Raman spectra of (a) 0.1, (b) 0.5, (c) 1 and (d) 10 mol% Fe doped  $TiO_2$ .

which was used for the precursor of Fe ion. When Fe concentration was more than 10 mol%, iron could not be intercalated completely into the  $TiO_2$ . At those contents,  $FeCl_3$  remained at the surface of  $TiO_2$ . The bands at 162 and 635  $cm^{-1}$  which were presented in all of the samples could be assigned to anatase  $TiO_2$  in agreement with XRD results in Fig. 2. However, pure  $TiO_2$  shows the characteristic band at 148  $cm^{-1}$  [Gotic et al., 1996]. The peak at 162  $cm^{-1}$  should be shifted from 148  $cm^{-1}$ . This shift to higher position in the Raman spectrum might be related to the decrease of particle size [Gotic et al., 1996]. In both of XRD and Raman spectra, any iron complex except the Fe precursor could not be found. This might be due to the good dispersion of Fe ion in the  $TiO_2$  lattice.

Tungsten-doped  $TiO_2$  nano particles showed different crystallographic results from iron-doped  $TiO_2$ . The XRD spectra of W-doped  $TiO_2$  in Fig. 4 presented anatase phase  $TiO_2$  and 12-tungstate. As the concentration of tungsten increased, 12-tungstate peak was decreased. It was confirmed by Raman spectra in Fig. 5. The bands at 160, 195 and 642  $cm^{-1}$  were assigned to anatase phase  $TiO_2$ . And, that of 960  $cm^{-1}$  was attributed to the 12-tungstate according to the reference [Scholz et al., 1999] and XRD results. Similarly with iron-doped  $TiO_2$ , the peak at 160  $cm^{-1}$  was supposed to be shifted from

Table 1. The mean particle sizes of pure  $TiO_2$  and metal doped  $TiO_2$  colloids

Dopant	Dopant concentration (mol%)				
	0 (Pure)	0.1	0.5	1	10
Fe	6 nm	4 nm	6 nm	6 nm	7 nm
W		5 nm	5 nm	4 nm	6 nm

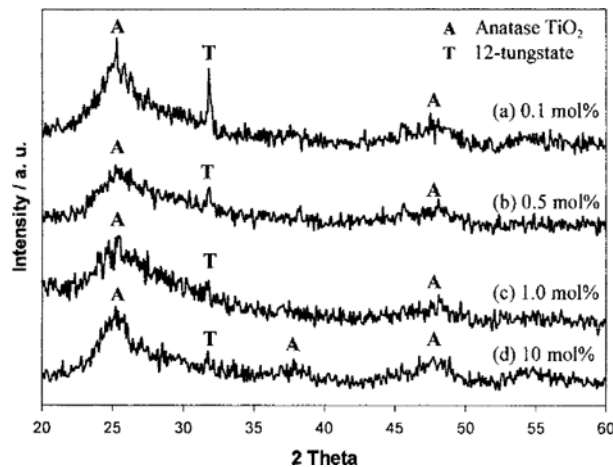


Fig. 4. XRD spectra of (a) 0.1, (b) 0.5, (c) 1 and (d) 10 mol% W doped  $\text{TiO}_2$ .

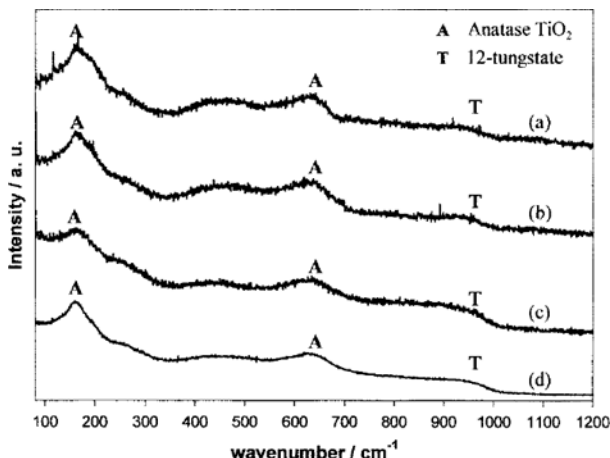


Fig. 5. Raman spectra of (a) 0.1, (b) 0.5, (c) 1 and (d) 10 mol% W doped  $\text{TiO}_2$ .

144  $\text{cm}^{-1}$ . This might also correspond to the reduction of  $\text{TiO}_2$  particle size. Because the tungsten oxide was detected in Raman and XRD spectroscopies, tungsten would be less dispersed than iron.

The photocatalytic oxidation using Fe- or W-doped  $\text{TiO}_2$  with various metal concentrations was evaluated on the basis of the photodegradation ratio of acetaldehyde. For the comparison of photocatalytic reaction rate, the pseudo 1st order reaction equation was introduced in this paper as follows.

$$\text{rate} = \frac{d[C]}{dt} = -k[C]$$

$$\ln \frac{[C]}{[C]_0} = -kt$$

where  $k$  is the apparent rate constant and  $[C]$  is the reactant concentration [Nimlos et al., 1996]. All of the photocatalytic reactions were well fitted to this pseudo 1st order reaction kinetics. Figs. 6 and 7 show the photocatalytic activity of metal doped titania with various concentrations of metals. As the concentration of W or Fe ion was increased, the reactivity was decreased. Although iron or tungsten precursor was not found by XRD and Raman spectra, high concentration of metal ion or surface metal oxide could hinder the

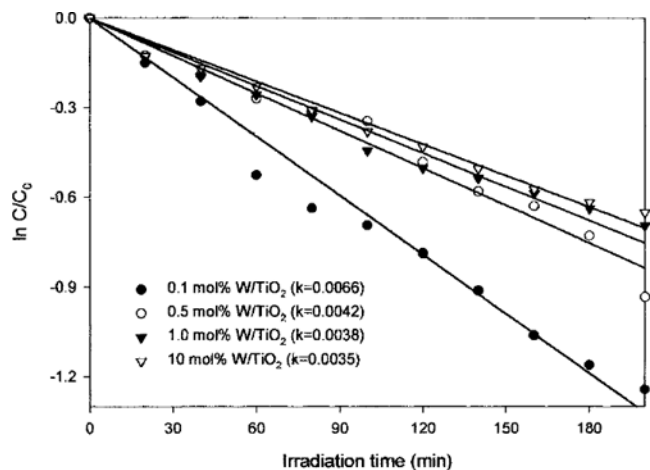


Fig. 6. Photocatalytic activity of 0.1, 0.5, 1, 10 mol% Fe doped  $\text{TiO}_2$  ( $k$  is rate constant).

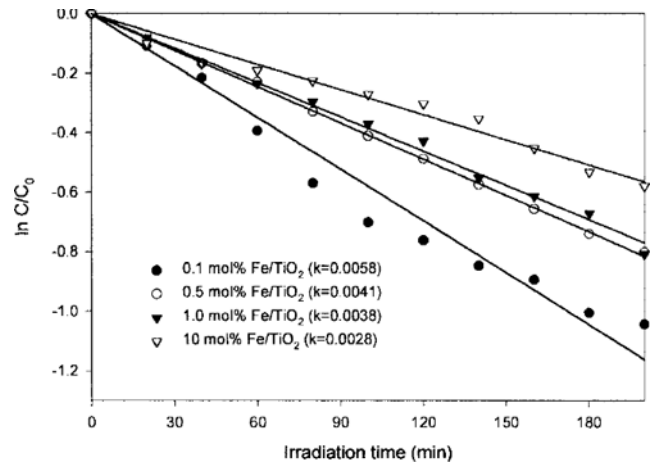


Fig. 7. Photocatalytic activity of 0.1, 0.5, 1, 10 mol% W doped  $\text{TiO}_2$  ( $k$  is rate constant).

photocatalytic process of  $\text{TiO}_2$ . These results are in agreement with other literature [Linsebigler et al., 1995; Litter et al., 1996]. The concentration of the beneficial transition metal dopants might be very small and large concentrations might be detrimental. According to Anpo et al., the surface-isolated metal ion species are active sites for the photocatalytic reaction. Only a low concentration of metal ion could form the isolated species on the surface of  $\text{TiO}_2$ . Therefore, the W and Fe contents were fixed at a very low concentration (0.1 mol%) which showed the highest reaction rate.

The photocatalytic activities of Fe- and W-doped  $\text{TiO}_2$  in Figs. 6 and 7 were lower than that of commercial  $\text{TiO}_2$ (P-25) of which the reaction constant was  $0.0170 \text{ min}^{-1}$ . It might be due to the low crystallinity of W- or Fe-doped  $\text{TiO}_2$  as shown in Figs. 2 and 4. To promote the crystallinity of  $\text{TiO}_2$ , the samples were sintered at 300 and 500 °C. The XRD patterns of 0.1 mol% iron-doped  $\text{TiO}_2$  with various calcination temperatures are shown in Fig. 8. There was no noticeable phase transformation with sintering duration. All the peaks were assigned to anatase  $\text{TiO}_2$  phase. As mentioned above, Fe ion was well dispersed in the  $\text{TiO}_2$  lattice. In the case of tungsten-doped  $\text{TiO}_2$ , however, some phase change occurred. The peak of 12-tungstate disappeared after heat treatment as shown in Fig. 9. And, titania

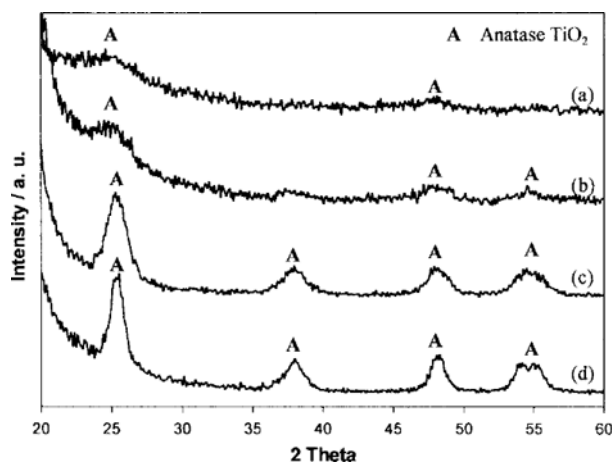


Fig. 8. XRD spectra of 0.1 mol% Fe/TiO<sub>2</sub> (a) uncalcined, and calcined at (b) 100 °C, (c) 300 °C and (d) 500 °C.

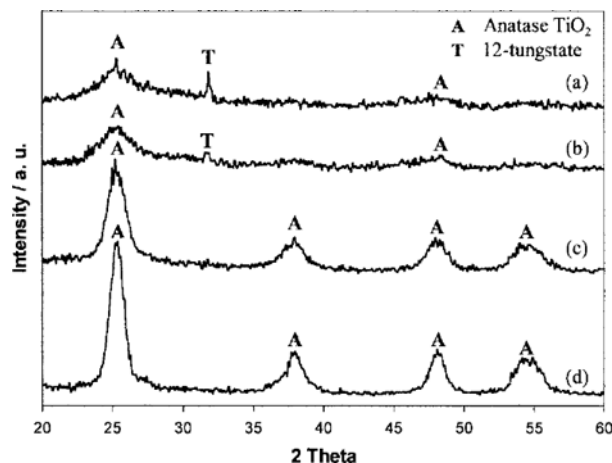


Fig. 9. XRD spectra of 0.1 mol% W/TiO<sub>2</sub> (a) uncalcined, and calcined at (b) 100 °C, (c) 300 °C and (d) 500 °C.

phase remained at anatase just as the iron-doped sample. The disappearance of 12-tungstate could be due to better dispersion of tungsten on the surface of TiO<sub>2</sub> and incorporation into the TiO<sub>2</sub> lattice by calcination process [Litter et al., 1996].

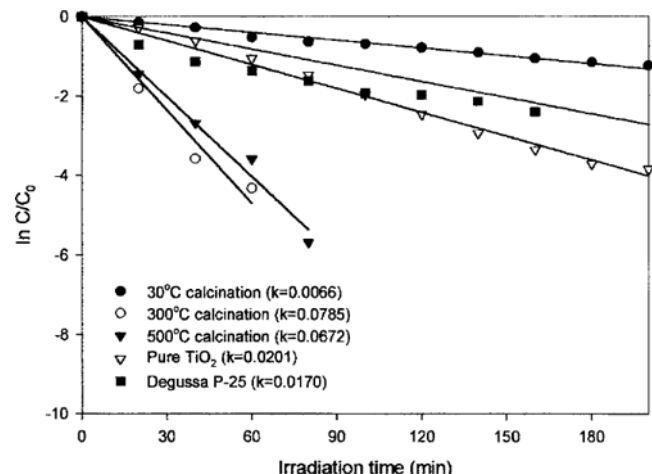


Fig. 11. Photocatalytic activity of 0.1 mol% W doped TiO<sub>2</sub>, pure TiO<sub>2</sub> and commercial TiO<sub>2</sub> ( $k$  is rate constant).

Figs. 10 and 11 show the photocatalytic activity of iron- and tungsten-doped TiO<sub>2</sub>. The reaction rate was drastically increased after 300 °C heat treatment. Furthermore, the photocatalytic activity of iron- or tungsten-doped TiO<sub>2</sub> was higher than that of synthesized pure TiO<sub>2</sub> and commercial TiO<sub>2</sub>. During the calcination, metal ion initially presented at the surface would diffuse into the lattice with increasing the crystallinity of TiO<sub>2</sub> [Litter et al., 1996]. This could promote the photocatalytic activity of metal-doped TiO<sub>2</sub>. However, in 500 °C sintering, photoreactivity of Fe- or W-doped TiO<sub>2</sub> was slightly decreased. Although the XRD spectra in Figs. 8 and 9 do not present any bulk iron oxide or tungsten oxide, iron oxide or tungsten oxide might lower the photocatalytic activity.

## CONCLUSION

All of the metal-doped titania prepared in this paper showed anatase phase of TiO<sub>2</sub>. For the iron- or tungsten-doped TiO<sub>2</sub>, any bulk phase was not found in both of XRD and Raman spectra at low loadings. It might be due to the good dispersion of Fe ion in the TiO<sub>2</sub> lattice. In the study of photocatalytic activity of metal-doped TiO<sub>2</sub>, as the concentration of W or Fe ion was increased, the reactivity was decreased. The reaction rate was drastically increased after 300 °C heat treatment. The photocatalytic activity of iron- or tungsten-doped TiO<sub>2</sub> was higher than that of commercial TiO<sub>2</sub>. By the sintering process, metal ion might easily enter the lattice with increasing the crystallinity of TiO<sub>2</sub>. It may promote the photocatalytic activity of TiO<sub>2</sub>.

## ACKNOWLEDGEMENT

This work was supported by the Brain Korea 21 Project, and Korean Institute of Environmental Science and Technology.

## REFERENCES

Anpo, M., Zhang, S. G., Mishima, H., Matsuoka, M. and Yamashita,

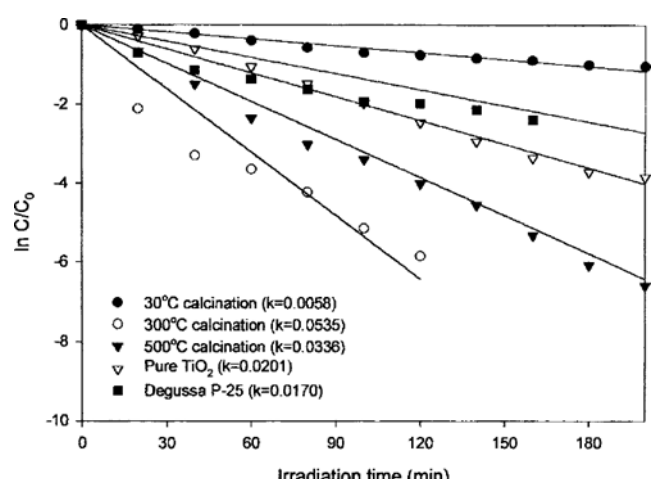


Fig. 10. Photocatalytic activity of 0.1 mol% Fe doped TiO<sub>2</sub>, pure TiO<sub>2</sub> and commercial TiO<sub>2</sub> ( $k$  is rate constant).

H., "Design of Photocatalysts Encapsulated within the Zeolite Framework and Cavities for the Decomposition of NO into N<sub>2</sub> and O<sub>2</sub> at Normal Temperature," *Catalysis Today*, **39**, 159 (1997).

Gotic, M., Ivanda, Sekulic, A., Music, S., Popovoic, S., Turkovic, A. and Furic, K., "Microstructure of Nanosized TiO<sub>2</sub> Obtained by Sol-Gel Synthesis," *Materials Letters*, **28**, 225 (1996).

Hoffmann, M. R., Martin, S. T., Choi, W. and Bahnemann, D. W., "Environmental Applications of Semiconductor Photocatalysis," *Chem. Rev.*, **95**, 69 (1995).

Linsebigler, A. L., Lu, G. and Yates, J. T., "Photocatalysis on TiO<sub>2</sub> Surface: Principles, Mechanisms, and Selected Results," *Chem. Rev.*, **95**, 735 (1995).

Litter, M. I. and Navio, J. A., "Photocatalytic Properties of Iron-Doped Titania Semiconductors," *J. Photochemistry and Photobiology A: Chemistry*, **98**, 171 (1996).

Mills, A. and Hunte, S. L., "An Overview of Semiconductor Photocatalysis," *J. Photochemistry and Photobiology A: Chemistry*, **108**, 1 (1997).

Nimlos, M. R., Wolfrum, E. J., Brewer, M. L., Fennell, J. A. and Bintner, G., "Gas Phase Heterogeneous Photocatalytic Oxidation of Ethanol: Pathways and Kinetic Modeling," *Environ. Sci. Technol.*, **30**, 3102 (1996).

Palmisano, L. and Sclafani, A., "Thermodynamics and Kinetics for Heterogeneous Photocatalytic Process," in *Heterogeneous Photocatalysis*, edited by M. Schiavello, John Wiley & Sons (1997).

Scholz, A., Schnyder, B. and Wokaun, A., "Influence of Calcination Treatment on the Structure of Grafted Wox Species on Titania," *J. Molecular Catalysis A: Chemical*, **138**, 249 (1999).

Zhang, Y., Xiong, G., Yao, Yang, W. and Fu, X., "Preparation of Titania-Based Catalysts for Formaldehyde Photocatalytic Oxidation from TiCl<sub>4</sub> by the Sol-Gel Method," *Catalysis Today*, **68**, 89 (2001).